analytical chemistry

May 7, 2019 Volume 91 Number 9

ACS Publications
Most Trusted. Most Cited. Most Read.

www.acs.org

analytical chemistry

Article

Cite This: Anal. Chem. 2019, 91, 5722−5728

pubs.acs.org/ac

Discovery of Turn-On Fluorescent Probes for Detecting Bcl-2 Protein

Tingting Liu,[†] Gaopan Dong,[†] Feng Xu,[†] Bo Han,[‡] Hao Fang,[†] Yun Huang,[§] Yubin Zhou,[§] Lupei Du,[†] and Minyong Li*[,†,∥]

[†]Department of Medicinal Chemistry, Key Laboratory of Chemical Biology (MOE), School of Pharmacy, Shandong University, Jinan, Shandong 250012, China

[‡]Department of Pathology, School of Medicine, Shandong University, Jinan, Shandong 250012, China

[§]Institute of Biosciences and Technology, College of Medicine, Texas A&M University, Houston, Texas 77030, United States

[∥]Helmholtz International Lab, State Key Laboratory of Microbial Technology, Shandong University, Jinan, Shandong 250100, China

Supporting Information

ABSTRACT: B-cell-lymphoma-2-gene (Bcl-2) family proteins play a central role in regulating programmed cell death. In cancer, antiapoptotic Bcl-2 proteins, such as Bcl-2 and Mcl-1, are overexpressed. However, there are few developed labeling techniques for tracing the dynamic processes of Bcl-2. To study the physiological process of Bcl-2 protein, a novel series of small-molecule fluorescent probes (**1**−**3**) were designed and evaluated for their labeling properties. Our probes can be applied to the identification of tumor-tissue slices and the differentiation of tumor and normal tissues effectively, a feature that renders these probes compatible with future cancer diagnosis in clinical practice.

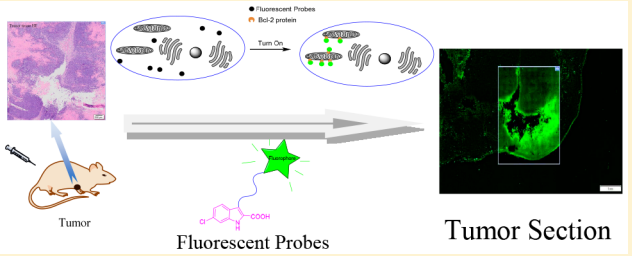

Proteins in the B-cell-lymphoma-2-gene (Bcl-2) family are major regulators of apoptosis. Overexpression of the prominent antiapoptotic Bcl-2-family members, including Bcl-2 and Mcl-1, is a common characteristics responsible for deregulation of apoptosis,[1] which makes cancer cells resistant to conventional tumor therapeutic agents and further results in hindrance of cancer-cell death. In addition, Bcl-2 overexpression can result in elevated vascular-endothelial-cell-growth-factor (VEGF) expression, which increases neo-angiogenesis of tumors in human-cancer xenografts.[2] Overall, Bcl-2 and Mcl-1 proteins appear to be attractive chemotherapeutic targets for the treatment of cancer.[3]

To aid the real-time monitoring and tracing of protein activities, several techniques have been developed, such as the use of fluorescence, radioisotopes, bioluminescence, and chemiluminescence. Recently, these techniques are applied as practical toolkits in the fields of pharmacological and physiological study, and each has its advantages. Therefore, on account of their special properties, such as convenient operation, high sensitivity, and flexibility, small-molecule fluorescent probes have been well-applied widely,[4−10] such as in labeling proteins by using bioorthogonal reactions,[11] which allows detection and imaging of enzymes, proteins,[12] channels,[13] RNA,[14] DNA,[15] receptors, and bioactive small molecules (H_2O_2, etc.)[16−20] and tracing the real-time processes in cellulo and in vivo. Moreover, some near-infrared probes could be applied to guiding surgery in clinical settings.[21−23] Accordingly, in analysis of Bcl-2-family proteins, a small-molecule fluorescent probe is expected to be a powerful toolkit to provide real-time and reliable information in living systems.

Few small-molecule fluorescent probes are available for detecting Bcl-2 proteins so far. Fortunately, a small-molecule fluorescent probe, **probe L**, was discovered for imaging and detecting Mcl-1 protein in our previous work.[24] Nevertheless, the binding affinity of this probe for Mcl-1 protein (IC_{50} = 16 ± 2.3 μM) needed to be improved. According to structural analysis of the lead compound, **probe L**,[25,26] the binding affinity of the compound relates to the substituent positions on the indolyl group. Therefore, the substituent position on the indolyl group was changed from the 1-position to the 3-position in the design of a new series of probes with an environment-sensitive turn-on mechanism. Moreover, the naphthyl group of the compound needed to be stretched into a deep hydrophobic pocket, because inadequate utilization of the full capacity of the hydrophobic pocket could limit its activity. Therefore, we suspected that replacing the naphthyl group with a substituent with a much larger volume would be beneficial for its hydrophobic interaction. At this point, a novel aggregation-induced-emission (AIE)-effect fluorophore, which was discovered by the Tang lab in 2001[27] and widely studied,[28−31] attracted us. Different from conventional fluorophores, AIEgen emits strongly in the aggregated state but is almost nonemissive in the molecular state. In aqueous media, this kind of fluorogen can be engineered to emit

Received: December 19, 2018
Accepted: March 12, 2019
Published: March 12, 2019

DOI: 10.1021/acs.analchem.8b05853
Anal. Chem. 2019, 91, 5722−5728

extremely weak fluorescence by endowing it with water solubility. Thus, it should be compatible with biological systems, with its fluorescence being turned on by interacting with target analytes.[32] From this point of view, a novel series of small-molecule fluorescent probes (**1**−**3**) was designed (Scheme 1).

Scheme 1. Design Strategy for Bcl-2−Mcl-1 Fluorescent Probes 1−3

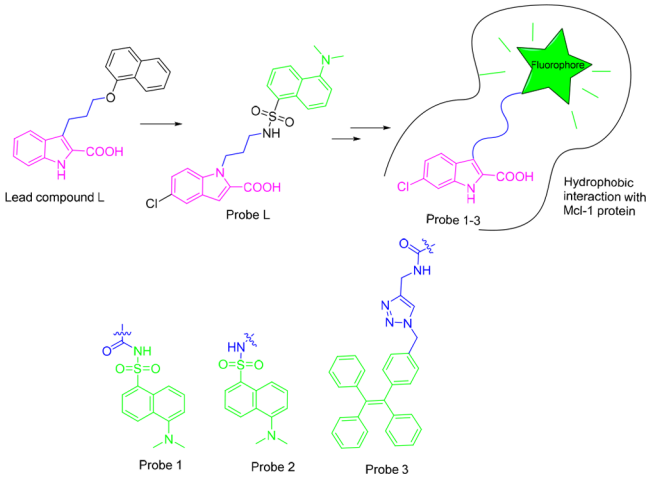

EXPERIMENTAL SECTION

Materials and Instruments. All reagents and solvents were used for chemical and biological experiments without further purification unless otherwise noted. Water used for cell experiments and fluorescence studies was doubly distilled. The melting points of the compounds were determined on a convenient electrothermal melting-point apparatus without correction. ^{1}H NMR and ^{13}C NMR of the products were recorded on a Bruker 400 MHz NMR spectrometer, using TMS as the internal standard. ESI-MS spectra were recorded by the analytical and mass-spectrometry facilities at the Shandong analysis and test center. Absorption and fluorescence spectra were recorded on Thermo Varioskan microplate reader. Fluorescence imaging was obtained by a Zeiss Axio Observer A1 fluorescence microscope and a Zeiss LSM780 confocal fluorescence microscope. HPLC examination of the compounds was performed on an Agilent 1260 HPLC system.

Fluorescence-Spectroscopy Test. The spectroscopic properties of probes **1**−**3** were determined in 10 μM solutions of PBS buffer (pH 7.4). Using a Thermo-Fisher Varioskan microplate reader, the fluorescent properties of probe **1**−**3** were determined. More details can be found in the Supporting Information.

Bcl-2-Inhibition Assay. The Bcl-2-protein-binding assays for probes **1**−**3** were performed by TR-FRET technology using a peptide-ligand substrate and recombinant Bcl-2 protein. The results were obtained by using a Tecan Infinite M1000 microplate reader. The fluorescence-polarization assay (FPA) was chosen for use in the binding assay for Mcl-1 protein and Bcl-xL protein. The experimental details were provided in the Supporting Information.

In Vitro Antiproliferative Assay. The cytotoxicity of the probes was determined by the sulforhodamine B (SRB) assay in K562, PC-3, HeLa, and MDA-MB-231 cells. In brief, 100 μL of culture medium containing 4.5 × 10^3 cells was added into each well of a 96-well plate and then cultured in 5% CO_2 atmosphere for 12 h at 37 °C. Subsequently, different concentrations (100 μL) of the samples were added into the wells. After a 48 h incubation, 100 μL of 10% (w/v) precooling trichloroacetic acid was added into the wells gently, and the plate was incubated at 4 °C for 1 h. The solvent of the plate was then removed, and the plate was washed with water three times. After it dried, 100 μL of SRB solution (4 g/L) was added into each well. After that, the plate was shaken for 30 min at 37 °C. The SRB solution of the plate was thrown away, and the plate was washed with 1% (v/v) acetic acid. Finally, 100 μL of 10 mM Tris-base solution was added, and the plate was shaken for 5 min; the absorbance values of the plates were recorded using a microplate reader at 515 nm, and the IC_{50} values were calculated.

Cell Staining and Fluorescence Imaging. HeLa and HEK293 cells were chosen for the fluorescence imaging. They were cultured in DMEM medium with 10% (v/v) fetal-bovine serum. When the cells were in exponential growth stage, they were seeded in confocal dishes and incubated for 12−24 h. After the medium was dropped away, the dishes were washed with RPMI-1640 medium gently. The concentrated solution (10 mM) of the test compound was diluted with RPMI-1640 medium. Subsequently, probes were incubated with HEK 293 and HeLa cells for 15 min, respectively. The competitive imaging assays were performed by incubating the positive control (10 μM AT-101) together with the probe (10 μM) at the same condition in HEK 293 and HeLa cells. Fluorescence imaging of these cells was performed on a Zeiss Axio Observer A1 fluorescence microscope (objective lens: 63×). Using the same procedure, probes **1** (10 μM) and **3** (40 μM) were costained with the commercial dyes MitoTracker Red CMXRos and Hoechst 33342. The fluorescence imaging was captured by a Zeiss LSM780 confocal fluorescence microscope.

Flow-Cytometry Analysis. The flow-cytometry tests of probes were performed on HeLa cells. At least 5 × 10^5 cells were collected and washed in 10 mM PBS three to four times. Probe **1** or **3** (final concentration of 10 μM) was added together with the positive control (10 μM AT-101) or solely into the flow tubes with 250 μL of PBS and 5 × 10^5 cells. Incubated for about half an hour under protection from light conditions, the tubes were analyzed by a BD FACSCalibur flow cytometer.

Fluorescence Imaging of Mouse Tumor and Normal Sections. To generate tumor xenografts in mice, HeLa cells (1 × 10^7) were implanted subcutaneously in the right and left armpit regions of 4−5 week old female nude mice. Tumors were allowed to grow to 1 cm^3. The tumors were separately made into paraffin slices, and the normal tissues were from the mouse thigh. Then, the sections were incubated with each probe (10 μM) or with each probe (10 μM) together with 10 μM AT-101 in Krebs solution at 4 °C overnight. After that, the sections were taken out and washed with Krebs solution once. After fixation of the sections, the imaging was performed immediately by an Olympus Imager fluorescence microscope (40×).

Immunohistochemical Experiments of Mouse Tumor and Normal Sections. Briefly, as described in previous article,[33,34] dewaxed sections of mouse tumor and normal tissues were microwaved for 15 min in 1× antigen-retrieval solution and, after proper cooling, were washed by being incubated with PBST twice for 5 min each; then, they were

DOI: 10.1021/acs.analchem.8b05853
Anal. Chem. 2019, 91, 5722−5728

incubated with nonspecific-staining-blocking agent for 10 min. After being washed with PBST twice, they were incubated overnight with the primary Bcl-2 antibody. After the overnight incubation with the primary antibody, the tissues were washed with PBST twice for 5 min. Then, the sections were incubated with the secondary Bcl-2 antibody for 30 min and washed with PBST three times for 7 min and then subsequently with the DAB kit for another 7 min. The reaction was stopped with water, and the sections were stained with hematoxylin and differentiated by hydrochloric alcohol. After fixation of the tumor and normal-tissue sections, imaging was performed immediately on an Olympus Imager fluorescence microscope (40×).

RESULTS AND DISCUSSION

Synthesis. Probes were synthesized through three routes, as shown in Schemes S1−S3. In the case of probe **1**, intermediate **8** was synthesized using *m*-chloroaniline and ethyl 2-oxocyclopentanecarboxylate as starting materials by a ring-opening reaction, esterification, a cyclization reaction, and a deprotection reaction. Naphthalene-sulfonyl chloride was converted into naphthalene sulfonamide (Scheme S1). Then, coupling intermediate **8** with compound **10** under HATU/DIEA conditions yielded key intermediate **11**. Finally, target compound **1** was obtained by de-ethylation of intermediate **11**. For probe **2** (Scheme S2), product **13** was synthesized by a condensation reaction with compound **8** and a reduction reaction with intermediate **12**. Afterward, it was condensed with naphthalene-sulfonyl chloride to give product **14**. After that, the ethyl group of compound **14** was removed to receive target compound **2**. For probe **3** (Scheme S3), the synthesis of compound **15** from product **8** and propargylamine involved coupling technology. Next, diphenylmethane reacted with 4-methylbenzophenone in the presence of *n*-butyllithium to give product **16**. Later, intermediate **19** was synthesized by a dehydration reaction, bromination, and a nucleophilic substitution reaction. Subsequently, intermediate **15** reacted with intermediate **19** in a click reaction, resulting in the crucial product, **20**. After the deprotection of **20**, we obtained target compound **3**. Further details on the synthesis and characterization of these probes can be found in the Supporting Information.

Spectroscopic Properties of Probes. As illustrated in Table 1, these probes possess efficient fluorescence properties.

Table 1. Photophysical Properties of Probes 1−3

probe	λ_{max} (nm)	λ_{ex} (nm)	λ_{em} (nm)	Φ (%)
1	300	305	535	42.16
2	302	305	545	7.95
3	304	310	488	1.70

In particular, probe **1** has an emission wavelength at 535 nm, and a relatively reasonable quantum yield of 42.16% (Table 1). Compared with probe **3**, the emission wavelengths of probes **1** and **2** are significantly red-shifted. The environment-sensitive effect of the dansyl fluorophore was studied in our previous study.[24] In addition, the novel AIE effect was studied using 10 μM solutions of probe **3** in different ratios of acetonitrile and PBS-solution mixture. As shown in Figure 1, solutions of probe **3** in acetonitrile, its suitable solvent, are nonemissive. Further, the addition of large amounts of 10 mM PBS into the acetonitrile solution of probe **3** causes the molecules to

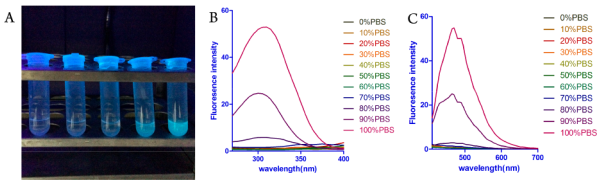

Figure 1. AIE effect of probe **3** studied in acetonitrile−PBS mixtures. (A) Left to right: 0, 70, 80, 90, and 100% PBS. (B,C) Excitation and emission spectra of probe **3**.

aggregate to induce emission efficiently, which is substantiated in terms of its spectroscopic properties and a TLC test: probe **3** can be induced to emit by aggregation. In other words, it is AIE-active, which is the same as the AIE effect reported by the Tang lab.

Cytotoxicity Assay. The cell viability of probes **1**−**3** was examined by a sulforhodamine B (SRB) method in PC-3, HeLa, K562, and MDA-MB-231 cells. As shown in Table 2, IC_{50} values of probes **1**−**3** were greater than 50 μM. Therefore, these results indicate that all probes demonstrate acceptable cell toxicity for detection and imaging of Bcl-2 proteins in living cells.

Bcl-2-Inhibiting Activity of Probes. The Bcl-2 inhibitory activities of these probes were well-evaluated, as listed in Table 3. Compared with our previously reported probe,[25] the binding affinity of probe **3** for Mcl-1 protein was improved. Furthermore, the experimental results also revealed that probes **1** and **3** had high affinities for Bcl-2 protein, which were comparable to that of the positive control, AT-101, and better than that of probe **2**; the importance of the amide bond to the activity could not be overstated. In particular, probe **3** can act on both Bcl-2 and Mcl-1 proteins. Therefore, we focused on evaluating the properties of probes **1** and **3**.

Fluorescent Properties of Probes Combined with Bcl-2 Protein and Nonspecific Protein (BSA). These probes were well-designed for Bcl-2-family proteins with a fluorescence turn-on mechanism. To confirm this, on the basis of the inhibitory-activity results, a series of concentrations of Bcl-2 or Mcl-1 protein solution was incubated with the same concentration of probes **1** and **3** (10 μM). As expected, the fluorescence intensities of these probes steadily heightened with increasing concentrations of Bcl-2-family proteins (Figure 2). Interestingly, the fluorescence intensity of probe **1** with 0.28 mg/mL Bcl-2 protein was 3.5-fold greater than that of the blank control group. When incubating probe **3** with 0.28 mg/mL Bcl-2 protein or 0.28 mg/mL Mcl-1 protein, the fluorescence intensity was 5.0- and 2.6-fold higher than that of the blank control group, respectively.

Subsequently, the selectivity of these probes was carefully examined. Bovine-serum albumin (BSA), a nonspecific binder of many molecules, was chosen as the negative control. Probe **1** (10 μM) was incubated with BSA or Bcl-2 at a concentration of 0.28 mg/mL, and probe **3** (10 μM) was incubated with BSA, Mcl-1, or Bcl-2 at a concentration of 0.28 mg/mL. Probe **1** presented a slightly higher fluorescence response when treated with Bcl-2 than when treated with BSA; nevertheless, probe **3** exhibited a much higher fluorescence response when treated with Bcl-2 or Mcl-1 than when treated with BSA. The most interesting result is that the response of probe **3** with Bcl-2 is 11-fold higher than that of the blank control with probe **3** only, 110-fold higher that of the blank control with Bcl-2 only (without probe **3**), and 5-fold higher that of BSA with probe **3**

DOI: 10.1021/acs.analchem.8b05853
Anal. Chem. 2019, 91, 5722−5728

Table 2. Cytotoxicity Results of Probes 1−3

probe	IC_{50} (μM)			
	HeLa cells	K562 cells	PC-3 cells	MDA-MB-231 cells
1	>100	>100	>100	>100
2	98.9 ± 0.07	89.1 ± 3.4	74.5 ± 1.8	89.9 ± 0.7
3	55.5 ± 1.3	>100	60.4 ± 1.6	61.2 ± 0.32
AT-101	9.9 ± 2.3	9.8 ± 2.6	11.3 ± 0.04	12.2 ± 0.98

Table 3. Inhibitory Activities of Compounds 1−3 against Bcl-2 Family Proteins

probe	IC_{50} (μM)		
	Bcl-2	Mcl-1	Bcl-xL
1	7.1 ± 0.00	NA	NA
2	35.1 ± 0.5	NA	NA
3	2.75 ± 0.64	2.9 ± 0.60	NA
AT-101	5.3 ± 0.17	2.1 ± 0.51	43.0 ± 8.7

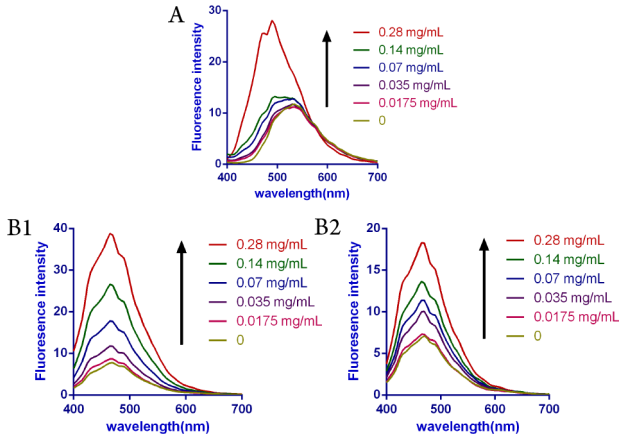

Figure 2. (A,B1) Fluorescence-emission spectra of (A) 10 μM probe **1** (λ_{ex} = 305 nm) and (B1) 10 μM probe **3** (λ_{ex} = 310 nm) incubated with six concentrations of Bcl-2 protein (0.28, 0.14, 0.07, 0.035, 0.0175, and 0 mg/mL) for about 20−30 min in the experimental buffer (50 mM Tris-HCl, 10 mM KCl, and 1 mM $MgCl_2$) at room temperature. (B2) Fluorescence-emission spectra of 10 μM probe **3** (λ_{ex} = 310 nm) incubated with six concentrations of Mcl-1 protein (0.28, 0.14, 0.07, 0.035, 0.0175, and 0 mg/mL).

(Figure 3). Moreover, the fluorescence intensities at the maximum emission wavelengths of these probes incubated with Bcl-2-family protein can be significantly reduced by an effective inhibitor, AT-101.

Fluorescence Imaging. Because probes **1** and **3** exhibit potent inhibitory activity, potent selectivity, excellent fluorescence properties, and acceptable cell toxicity, they were selected as suitable candidates for labeling Bcl-2-family proteins. Subsequently, the selectivity of probes **1** and **3** for Bcl-2 protein in living cells was evaluated by using HeLa and HEK 293 cells. The experimental results demonstrated that these probes can emit strong fluorescence and respond to HeLa cells rapidly (Figures 4 and 5). As the negative control, the inhibition of Bcl-2 protein was tested by incubating HeLa cells with 10 μM AT-101, and HEK 293 cells were chosen for imaging incubation with each probe. Inhibition of Bcl-2 protein by AT-101 resulted in an obvious decrease of fluorescence intensity. Moreover, the imaging using HEK293 cells showed weaker fluorescence compared with that of the imaging using HeLa cells. Therefore, both probes display

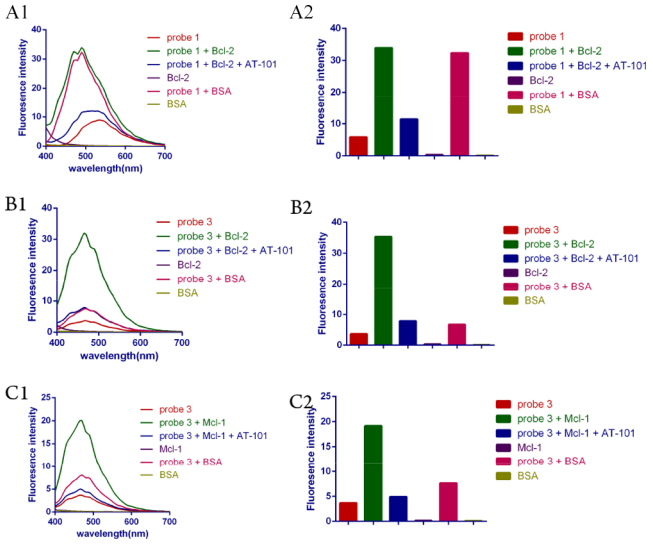

Figure 3. (A1,B1,C1) Fluorescence-emission spectra of 10 μM probe **1** or **3**, 0.28 mg/mL Bcl-2 or Mcl-1, 0.28 mg/mL BSA, probe with Bcl-2 or Mcl-1, probe with Bcl-2 or Mcl-1 and 10 μM AT-101, and probe with BSA incubated for 15−30 min in buffer (50 mM Tris-HCl, 1 mM $MgCl_2$, and 10 mM KCl) at room temperature. (A2,B2,C2) Column graphs of the fluorescence intensities of 10 μM probe **1** (490 nm) or **3** (465 nm), 0.28 mg/mL Bcl-2 or Mcl-1, 0.28 mg/mL BSA, probe with Bcl-2 or Mcl-1, probe with Bcl-2 or Mcl-1 and 10 μM AT-101, and probe with BSA. (A) Probe **1** with Bcl-2, (B) probe **3** with Bcl-2, and (C) probe **3** with Mcl-1.

favorable selectivity for Bcl-2-family protein and could be used in Bcl-2-family-protein detection.

Additionally, in order to analyze the active sites of the probes with Bcl-2-family proteins, the colocalization of probes **1** and **3** with the Bcl-2-family proteins was studied. We hypothesized that our probes colocalized with Bcl-2-family proteins at their interaction site. To validate this hypothesis, our probes were costained with the commercial dyes MitoTracker Red CMXRos (for mitochondria) and Hoechst 33342 (for nuclei) as presented in Figures 6 and 7. It is well-known that Bcl-2-family proteins are generally located in cytoplasm (mostly in mitochondria). The results demonstrated that the protein marked by these two probes was positioned in cytoplasm (primarily in mitochondria) rather than in the nucleus, which was consistent with our hypothesis. Furthermore, it is worth mentioning that all cell images were taken in the absence of a washing procedure after incubation, which enabled specific and real-time tracking of the protein without background interference. These attractive occurrences are due to the off−on mechanism of the fluorophores.

Flow-Cytometry (FCM) Assay. Thenceforward, to further study the binding of these probes to HeLa cells, a flow-cytometry assay was chosen for this study (Figure 8). It was obvious that the binding of our probes to Bcl-2-family proteins in HeLa cells was much higher than the nonspecific binding in

DOI: 10.1021/acs.analchem.8b05853
Anal. Chem. 2019, 91, 5722−5728

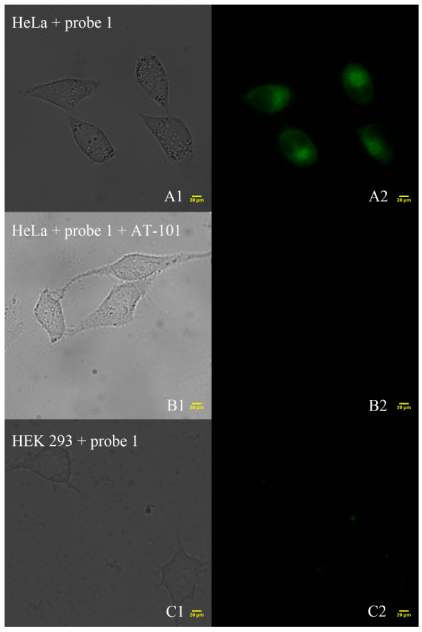

Figure 4. (A1,B1,C1) Bright-field and (A2,B2,C2) fluorescence (GFP channel) imaging of (A) 10 μM probe **1** in HeLa cells, (B) 10 μM AT-101 with 10 μM probe **1** in HeLa cells, and (C) 10 μM probe **1** in HEK293 cells. HEK293 and HeLa cells were incubated with the probes at 37 °C for 15 min. Objective lens: 63×.

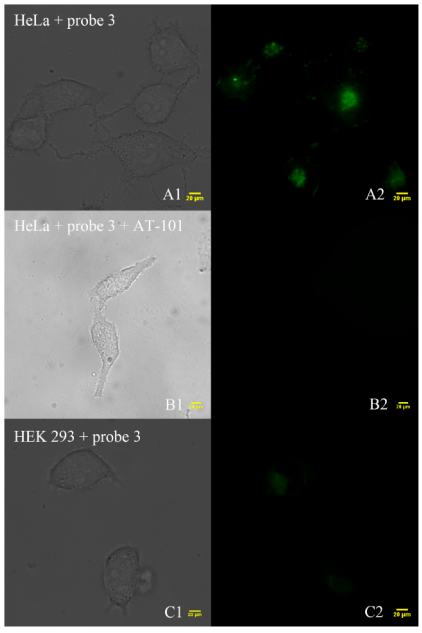

Figure 5. (A1,B1,C1) Bright-field and (A2,B2,C2) fluorescence (GFP channel) imaging of (A) 10 μM probe **3** in HeLa cells, (B) 10 μM AT-101 with 10 μM probe **3** in HeLa cells, and (C) 10 μM probe **3** in HEK293 cells.

HeLa cells treated with our probes and AT-101. Furthermore, the binding of probe **3** to HeLa cells was a little higher than that of probe **1**, which was consistent with the results that probe **3** displayed better inhibitory activities. More details are presented in the Experimental Section.

Hematoxylin−Eosin (HE) and Immunohistochemical (IHC) Experiments. To study the ability of probes **1** and **3** in Bcl-2-targeted imaging, a subcutaneous HeLa-xenograft mouse

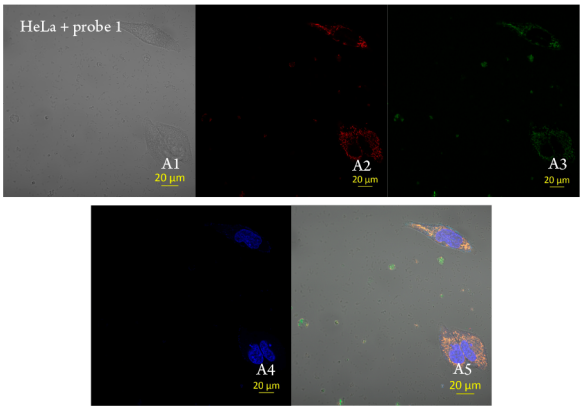

Figure 6. (A1) Bright-field and (A2,A3,A4) fluorescence (green channel) imaging of HeLa cells with (A2) MitoTracker Red CMXRos (mitochondrial dye), (A3) 10 μM probe **1**, and (A4) Hoechst 33342 (nuclear dye). (A5) Merged image. Images were obtained from a Zeiss LSM780 confocal fluorescence microscope.

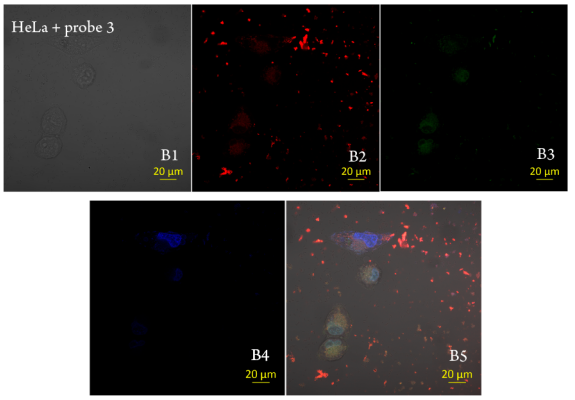

Figure 7. (B1) Bright-field and (B2,B3,B4) fluorescence (green channel) imaging of HeLa cells with (B2) MitoTracker Red CMXRos (mitochondrial dye), (B3) 40 μM probe **3**, and (B4) Hoechst 33342 (nuclear dye). (B5) Merged image.

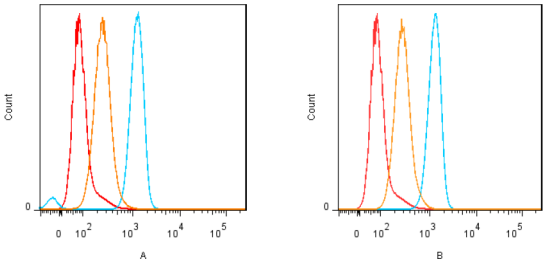

Figure 8. Flow-cytometry results of (A) 10 μM probe **1** and (B) 10 μM probe **3** with and without 10 μM AT-101 in living HeLa cells. Red: blank, yellow: probe **1** or **3** with AT-101, blue: probe **1** or **3** only.

model was established. Then, the tumors were separately made into paraffin slices. Hematoxylin−eosin (HE) staining was carried out by using sections provided by Shandong University Qilu Hospital. The results indicated that compared with the normal mouse tissue, the mouse tumor sections exhibited pathological conditions (Figure 9). Furthermore, in order to study the expression level of Bcl-2 protein and the tissue-specific distribution of Bcl-2-family protein in these tissues, an immunohistochemical (IHC) experiment with Bcl-2 antibodies was carried out. As shown in Figure 10, compared with the

DOI: 10.1021/acs.analchem.8b05853
Anal. Chem. 2019, 91, 5722−5728

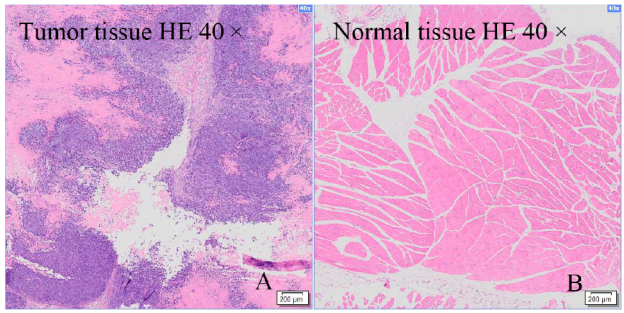

Figure 9. Hematoxylin−eosin staining of (A) tumor tissue and (B) normal tissue. Imaging was performed using an Olympus Imager fluorescence microscope (40×).

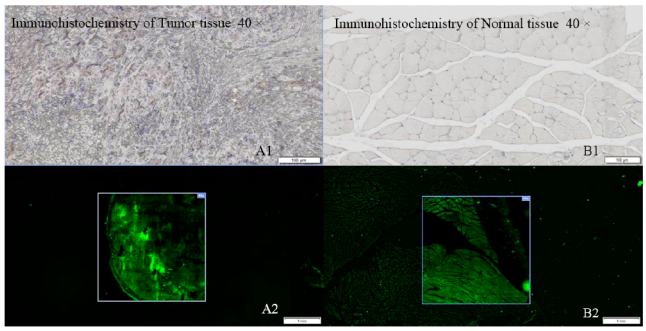

Figure 10. Immunohistochemical experiments. Immunohistochemistry of (A) tumor-tissue sections and (B) normal-tissue sections with Bcl-2 antibody. (A1,B1) Bright field. (A2,B2) Green channel. Imaging was performed using an Olympus Imager fluorescence microscope (40×).

normal-tissue section (Figure 10B), the tumor-tissue section was more effectively stained by the Bcl-2 antibody (Figure 10A), and the fluorescence intensity of the tumor section was stronger. These interesting results demonstrated that the tumor tissues overexpressed Bcl-2 proteins compared with the normal tissue, which is consistent with the fact that Bcl-2-family proteins are overexpressed in cancers. Therefore, these sections could be well-applied for probe-imaging assays.

In order to verify whether our probes could selectively label the Bcl-2 proteins as well as identify the tumor site, imaging assays were carried out on sections of these tissues. After a 24 h incubation with 10 μM probe **1** or **3** with 10 μM AT-101 (more details can be found in the Experimental Section), the tumor sections (Figure 11A,B) with probe had stronger fluorescence than those with probe and AT-101 (Figure 11C,D). Moreover, the fluorescence intensities of the tumor sections with probe were stronger than those of the normal sections with probe (Figure 11E,F). More interestingly, tumor tissue with higher malignancy showed much stronger fluorescence than tumor tissue with lower malignancy (Figure 11A,B), which indicated that sites of relatively high levels of tumor can be significantly marked by our probes, in contrast to the experimental results with the Bcl-2 antibody (Figure 10A2). This amazing result revealed that these probes may be used as an effective toolkit for cancer diagnosis in clinical practice.

CONCLUSION

We have designed a series of off−on small-molecule fluorescent probes (**1**−**3**) with excellent fluorescent properties

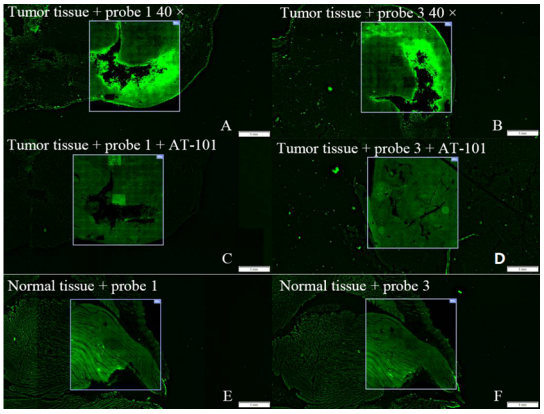

Figure 11. (A,B) Fluorescence-microscopy imaging (GFP channel) of tumor sections incubated with 10 μM probe. (C,D) Fluorescence-microscopy imaging of the inhibition of Bcl-2 protein in tumor sections accomplished by incubating 100 μM AT-101 with 10 μM probe. (E,F) Fluorescence-microscopy imaging of normal sections incubated with 10 μM probe. (A,C,E) Probe **1**. (B,D,F) Probe **3**. Imaging was performed using an Olympus Imager fluorescence microscope (40×).

for Bcl-2 visualization. Once these probes bind to the Bcl-2 proteins, they release strong fluorescence. Fortunately, probes **1** and **3** exhibit potent inhibitory activity against Bcl-2 proteins at levels that are comparable to that of the positive control, AT-101; nevertheless, probe **3** shows better selectivity for Bcl-2 and Mcl-1 proteins. Moreover, preparation of these probes is convenient and affordable. More importantly, probes **1** and **3** were successfully applied for the detection of tumor-tissue slices, and the imaging results of the tumor and normal tissues presented obvious differences. Compared with the Bcl-2 antibody, the visualization of tissues using probes **1** and **3** is much more convenient. Therefore, these small-molecule fluorescent probes can be further employed as a powerful fluorogenic tool in drug screening and cell staining in Bcl-2 fields, as well as in pathological and physiological studies of Bcl-2-family proteins.

ASSOCIATED CONTENT

Supporting Information

The Supporting Information is available free of charge on the ACS Publications website at DOI: 10.1021/acs.analchem.8b05853.

Synthetic procedures, fluorescence-spectroscopy test, and original spectra for structural characterization (PDF)

AUTHOR INFORMATION

Corresponding Author

*Tel. and Fax: +86-531-8838-2076. E-mail: mli@sdu.edu.cn.

ORCID

Hao Fang: 0000-0002-2879-5146
Yubin Zhou: 0000-0001-7962-0517
Lupei Du: 0000-0003-0531-8985
Minyong Li: 0000-0003-3276-4921

Author Contributions

The final manuscript was approved by all authors.

Notes

The authors declare no competing financial interest.

DOI: 10.1021/acs.analchem.8b05853
Anal. Chem. 2019, 91, 5722−5728

■ ACKNOWLEDGMENTS

This work was supported by grants from the Shandong Natural Science Foundation (No. ZR2018ZC0233), the Taishan Scholar Program at Shandong Province, the Qilu/Tang Scholar Program at Shandong University, the Key Research and Development Project of Shandong Province (No. 2017CXGC1401), and the Major Project of Science and Technology of Shandong Province (No. 2015ZDJS04001).

■ REFERENCES

(1) Oltersdorf, T.; Elmore, S. W.; Shoemaker, A. R.; Armstrong, R. C.; Augeri, D. J.; Belli, B. A.; Bruncko, M.; Deckwerth, T. L.; Dinges, J.; Hajduk, P. J.; et al. *Nature* **2005**, *435*, 677−681.
(2) Biroccio, A.; Candiloro, A.; Mottolese, M.; Sapora, O.; Albini, A.; Zupi, G.; Del Bufalo, D. *FASEB J.* **2000**, *14*, 652−660.
(3) Hata, A. N.; Engelman, J. A.; Faber, A. C. *Cancer Discovery* **2015**, *5*, 475−487.
(4) Liu, T.; Jiang, Y.; Liu, Z.; Li, J.; Fang, K.; Zhuang, C.; Du, L.; Fang, H.; Sheng, C.; Li, M. *MedChemComm* **2017**, *8*, 1727−1731.
(5) Liu, Z.; Miao, Z.; Li, J.; Fang, K.; Zhuang, C.; Du, L.; Sheng, C.; Li, M. *Chem. Biol. Drug Des.* **2015**, *85*, 411−417.
(6) Ma, Z.; Lin, Y.; Cheng, Y.; Wu, W.; Cai, R.; Chen, S.; Shi, B.; Han, B.; Shi, X.; Zhou, Y.; et al. *J. Med. Chem.* **2016**, *59*, 2151−2162.
(7) Qi, J.; Chen, C.; Zhang, X.; Hu, X.; Ji, S.; Kwok, R. T. K.; Lam, J. W. Y.; Ding, D.; Tang, B. Z. *Nat. Commun.* **2018**, *9*, 1848.
(8) Liu, Z.; Jiang, T.; Wang, B.; Ke, B.; Zhou, Y.; Du, L.; Li, M. *Anal. Chem.* **2016**, *88*, 1511−1515.
(9) Liu, J.; Tian, C.; Jiang, T.; Gao, Y.; Zhou, Y.; Li, M.; Du, L. *ACS Med. Chem. Lett.* **2017**, *8*, 428−432.
(10) Yuan, L.; Lin, W.; Zheng, K.; Zhu, S. *Acc. Chem. Res.* **2013**, *46*, 1462−1473.
(11) Takaoka, Y.; Ojida, A.; Hamachi, I. *Angew. Chem., Int. Ed.* **2013**, *52*, 4088−4106.
(12) Liu, Y.; Zhang, X.; Tan, Y. L.; Bhabha, G.; Ekiert, D. C.; Kipnis, Y.; Bjelic, S.; Baker, D.; Kelly, J. W. *J. Am. Chem. Soc.* **2014**, *136*, 13102−13105.
(13) Lougheed, T.; Borisenko, V.; Hand, C. E.; Woolley, G. A. *Bioconjugate Chem.* **2001**, *12*, 594−602.
(14) Sato, S.; Watanabe, M.; Katsuda, Y.; Murata, A.; Wang, D. O.; Uesugi, M. *Angew. Chem., Int. Ed.* **2015**, *54*, 1855−1858.
(15) Yasmeen, A.; Du, F.; Zhao, Y.; Dong, J.; Chen, H.; Huang, X.; Cui, X.; Tang, Z. *ACS Chem. Biol.* **2016**, *11*, 1945−1951.
(16) Lippert, A. R.; New, E. J.; Chang, C. J. *J. Am. Chem. Soc.* **2011**, *133*, 10078−10080.
(17) Ueno, T.; Nagano, T. *Nat. Methods* **2011**, *8*, 642−645.
(18) Chan, J.; Dodani, S. C.; Chang, C. *Nat. Chem.* **2012**, *4*, 973−984.
(19) Chen, X.; Tian, X.; Shin, I.; Yoon, J. *Chem. Soc. Rev.* **2011**, *40*, 4783−4804.
(20) Giepmans, B. N.; Adams, S. R.; Ellisman, M. H.; Tsien, R. Y. *Science* **2006**, *312*, 217−224.
(21) Choi, H. S.; Gibbs, S. L.; Lee, J. H.; Kim, S. H.; Ashitate, Y.; Liu, F.; Hyun, H.; Park, G. L.; Xie, Y.; Bae, S.; et al. *Nat. Biotechnol.* **2013**, *31*, 148−153.
(22) Antaris, A. L.; Chen, H.; Diao, S.; Ma, Z.; Zhang, Z.; Zhu, S.; Wang, J.; Lozano, A. X.; Fan, Q.; Chew, L.; et al. *Nat. Commun.* **2017**, *8*, 15269.
(23) Ni, X.; Zhang, X.; Duan, X.; Zheng, H. L.; Xue, X. S.; Ding, D. *Nano Lett.* **2019**, *19*, 318.
(24) Liu, T.; Gao, Y.; Zhang, X.; Wan, Y.; Du, L.; Fang, H.; Li, M. *Anal. Chem.* **2017**, *89*, 11173−11177.
(25) Friberg, A.; Vigil, D.; Zhao, B.; Daniels, R. N.; Burke, J. P.; Garciabarrantes, P. M.; Camper, D. M.; Chauder, B. A.; Lee, T.; Olejniczak, E. T.; et al. *J. Med. Chem.* **2013**, *56*, 15−30.
(26) Wan, Y.; Dai, N.; Tang, Z.; Fang, H. *Eur. J. Med. Chem.* **2018**, *146*, 471−482.
(27) Hong, Y.; Lam, J. W. Y.; Tang, B. Z. *Chem. Commun.* **2009**, *45*, 4332−4353.
(28) Dhara, K.; Hori, Y.; Baba, R.; Kikuchi, K. *Chem. Commun.* **2012**, *48*, 11534−11536.
(29) Kwok, R. T.; Leung, C. W.; Lam, J. W.; Tang, B. Z. *Chem. Soc. Rev.* **2015**, *44*, 4228−4238.
(30) Gao, H.; Zhang, X.; Chen, C.; Li, K.; Ding, D. *Adv. Biosys.* **2018**, *2*, e1800074.
(31) Qi, J.; Chen, C.; Ding, D.; Tang, B. Z. *Adv. Healthcare Mater.* **2018**, *7*, e1800477.
(32) Liang, J.; Tang, B. Z.; Liu, B. *Chem. Soc. Rev.* **2015**, *44*, 2798−2811.
(33) Dou, Z.; Ghosh, K.; Vizioli, M. G.; Zhu, J.; Sen, P.; Wangensteen, K. J.; Simithy, J.; Lan, Y.; Lin, Y.; Zhou, Z. *Nature* **2017**, *550*, 402−406.
(34) Dall'Aglio, C.; Polisca, A.; Cappai, M. G.; Mercati, F.; Troisi, A.; Pirino, C.; Scocco, P.; Maranesi, M. *Eur. J. Histochem.* **2017**, *61*, 2761−2764.

DOI: 10.1021/acs.analchem.8b05853
Anal. Chem. 2019, 91, 5722−5728